8-1-2012

Conversion of human 5-lipoxygenase to a 15-lipoxygenase by a point mutation to mimic phosphorylation at Serine-663

Nathaniel C. Gilbert
Louisiana State University

Zhe Rui
Louisiana State University

David B. Neau
Argonne National Laboratory

Maria T. Waight
Louisiana State University

Sue G. Bartlett
Louisiana State University

See next page for additional authors

Recommended Citation

Gilbert, N., Rui, Z., Neau, D., Waight, M., Bartlett, S., Boeglin, W., Brash, A., & Newcomer, M. (2012). Conversion of human 5-lipoxygenase to a 15-lipoxygenase by a point mutation to mimic phosphorylation at Serine-663. *FASEB Journal, 26* (8), 3222-3229. https://doi.org/10.1096/fj.12-205286

Conversion of human 5-lipoxygenase to a 15-lipoxygenase by a point mutation to mimic phosphorylation at Serine-663

Nathaniel C. Gilbert,* Zhe Rui,* David B. Neau,† Maria T. Waight,* Sue G. Bartlett,* William E. Boeglin,‡,§ Alan R. Brash,‡,§ and Marcia E. Newcomer*,1

*Department of Biological Sciences, Louisiana State University, Baton Rouge, Louisiana, USA; †Northeastern Collaborative Access Team, Argonne National Laboratory, Argonne, Illinois, USA; and ‡Department of Pharmacology and §Vanderbilt Institute for Chemical Biology, Vanderbilt University, Nashville, Tennessee

ABSTRACT **The enzyme 5-lipoxygenase (5-LOX) initiates biosynthesis of the proinflammatory leukotriene lipid mediators and, together with 15-LOX, is also required for synthesis of the anti-inflammatory lipoxins. The catalytic activity of 5-LOX is regulated through multiple mechanisms, including Ca^{2+}-targeted membrane binding and phosphorylation at specific serine residues. To investigate the consequences of phosphorylation at S663, we mutated the residue to the phosphorylation mimic Asp, providing a homogenous preparation suitable for catalytic and structural studies. The S663D enzyme exhibits robust 15-LOX activity, as determined by spectrophotometric and HPLC analyses, with only traces of 5-LOX activity remaining; synthesis of the anti-inflammatory lipoxin A_4 from arachidonic acid is also detected. The crystal structure of the S663D mutant in the absence and presence of arachidonic acid (in the context of the previously reported Stable-5-LOX) reveals substantial remodeling of helices that define the active site so that the once fully encapsulated catalytic machinery is solvent accessible. Our results suggest that phosphorylation of 5-LOX at S663 could not only down-regulate leukotriene synthesis but also stimulate lipoxin production in inflammatory cells that do not express 15-LOX, thus redirecting lipid mediator biosynthesis to the production of proresolving mediators of inflammation.—Gilbert, N. C., Rui, Z., Neau, D. B., Waight, M. T., Bartlett, S. G., Boeglin, W. E., Brash, A. R., Newcomer, M. E. Conversion of human 5-lipoxygenase to a 15-lipoxygenase by a point mutation to mimic phosphorylation at Serine-663. *FASEB J.* 26, 3222–3229 (2012). www.fasebj.org**

Key Words: leukotrienes · crystal structure · crystallography · eicosanoids

Leukotrienes (LTs) are potent mediators of the inflammatory response derived from arachidonic acid (AA). On leukocyte activation, AA is released from the nuclear membrane by the action of cytosolic phospholipase A_2 and binds 5-lipoxygenase-activating protein (FLAP). The increased Ca^{2+} concentration of the activated cells simultaneously promotes translocation of 5-lipoxygenase (5-LOX) to the nuclear membrane, where it acquires its substrate from FLAP (1, 2). AA is converted to leukotriene A_4 (LTA_4) in a 2-step reaction that produces the 5*S*-isomer of hydroperoxyeicosatetraenoic acid (5*S*-HPETE) as an intermediate (3, 4). While 5-LOX production of LTA_4 promotes inflammation, 5-LOX is also required for the synthesis of the lipoxins (LXs) (5, 6), structurally related compounds with anti-inflammatory properties that promote resolution of inflammation. LXs are the products of successive LOX reactions. For example LXA_4 is synthesized by the actions of both 15-LOX and 5-LOX. 15-LOX generates 15*S*-HPETE, which serves as a substrate for 5-LOX; 5-LOX converts the 15-LOX product to LXA_4. 15-LOX and 5-LOX are generally not present in the same cell types and LX synthesis has been reported to be transcellular (7–10).

LT production is regulated by phosphorylation of 5-LOX, and 3 kinase-targeted sites have been reported: Ser-271, Ser-523, and Ser-663 (11–15). S663 has been shown to be a substrate for ERK2 *in vitro* (11–13, 16), and its phosphorylation is thought to lead to increased enzyme activity (12). Paradoxically, 5-LOX product formation has been observed to be depressed in cells in which ERK2 activity is up-regulated (17). To understand the structural basis for altered LT production as a consequence of phosphorylation at S663, we prepared the S663D mutant of 5-LOX to mimic the phosphorylated state. The mutation of a Ser to an Asp is a well-established method to approximate the phosphorylated form of an enzyme for studies that require a homogenous sample of the modified enzyme (18). The

Abbreviations: 5-LOX, 5-lipoxygenase; AA, arachidonic acid; DGLA, dihomo-γ-linolenic acid; HPETE, hydroperoxyeicosatetraenoic acid; LOX, lipoxygenase; LT, leukotriene; LX, lipoxin; NAGly, *N*-arachidonyl glycine

[1] Correspondence: Department of Biological Sciences, Louisiana State University, Baton Rouge, LA 70803, USA. E-mail: newcomer@lsu.edu

doi: 10.1096/fj.12-205286

This article includes supplemental data. Please visit *http://www.fasebj.org* to obtain this information.

0892-6638/12/0026-3222 © FASEB

mutation was made in the context of Stable-5-LOX, a soluble 5-LOX that lacks putative membrane insertion residues and retains wild-type activity (19). The crystal structure of the S663D-Stable-5-LOX was determined in the absence and presence of substrate. The crystal structure of the enzyme with AA, combined with both altered substrate and product profiles for the modified enzyme, lead us to suggest that phosphorylation of 5-LOX at S663 converts the enzyme to a robust 15-LOX. Moreover, the same mutation in the context of the wild-type enzyme also results in 15-LOX activity. Our data suggest that the phosphorylation of 5-LOX at S663 can both down-regulate production of proinflammatory LTs and stimulate production of antiinflammatory LXs in cells which do not express 15-LOX.

MATERIALS AND METHODS

Construction of plasmid for protein expression

The 5-LOX insert in pCR2.1 was amplified by the polymerase chain reaction, cloned into pET28b (Novagen, San Diego, CA, USA), and then subcloned into pET14b for leaky expression. Mutations were constructed using whole-plasmid PCR (20). Primers were constructed to contain silent mutations that facilitated screening of plasmids. Small-scale expression to assess expression levels and solubility of the various mutant 5-LOXs was carried out by autoinduction (21).

Protein expression and purification

Protein was expressed and purified as described previously for Stable 5-LOX (19). Purification of the wild-type enzyme harboring the S663D mutation required 0.5% dodecyl maltoside in the lysis buffer. Assays for product specificity for that enzyme were preformed with the protein that eluted from the Ni-NTA column. No detergent was used for either the Stable-5-LOX S663D or S663A mutant purifications, or that of the parent enzyme.

Enzyme assays

Stable-5-LOX and its S663D mutant were assayed by monitoring the increase in absorbance at 238 nm in an Agilent 8453 Diode Array Spectrophotometer (Agilent Technologies, Santa Clara, CA, USA). The different substrates AA, dihomo-γ-linolenic acid (DGLA), and *N*-arachidonyl glycine (NAGly) were diluted to 10 mM in 100% ethanol or dimethyl sulfoxide. Assays were performed in 20 mM Tris-HCl (pH 7.5) and 150 mM NaCl with 140 nM enzyme. The concentration of substrates was varied from 1.5 to 30 μM for the determination of kinetic parameters.

The products of the reaction mixtures were identified from incubations as described previously (19). Briefly, the reaction was initiated by addition of AA (10–100 μM) added in 1–5 μl ethanol and monitored by UV spectroscopy until completion. Products were extracted by adjusting the solution to ~pH 4 by addition of 50 μl 1 M KH_2PO_4 plus 5 μl 1N HCl and vigorous mixing with 2 vol of dichloromethane. After a brief centrifugation to clear the phases, the lower organic layer was collected, washed twice with 0.5 ml water, taken to dryness under a stream of nitrogen, and then dissolved in a small volume of methanol for storage at −20°C. Prior to HPLC, peroxides were reduced by the addition of triphenylphosphine. Thus, the elution times are for the hydroxyproducts (HETEs), rather than the HPETEs. Reversed-phase HPLC was performed using Agilent 1100 series equipment with a Waters C18 Symmetry column (25×0.46 cm; Waters Corp., Milford, MA, USA) or a Dionex HPLC with a diode array detector (Dionex, Sunnyvale, CA, USA) and a Discovery HS C18 column. The mobile phase was acetonitrile/water/formic acid (60:40:0.01, v/v/v) or methanol/water/glacial acetic acid (80:20:0.01, v/v/v). The chirality of the product was confirmed as 5*S* or 15*S* by chromatography on a Chiralpak AD column (4.6×250 mm; Chiral Technologies, Inc., West Chester, PA, USA) with a mobile phase of hexane/methanol (100:2) at a flow rate of 1 ml/min. The HETEs were converted to the methyl esters before chiral analysis using ethereal diazomethane.

LX assays

The products of the coincubation of S663D-Stable-5-LOX and Stable-5-LOX were extracted as above and separated by reverse-phase HPLC. The mobile phase varied from acetonitrile/water/formic acid at 20:80:0.01 to 60:40:0.01 over 20 ml. Enzymes (at 1 μM) were incubated with 70 μM AA for 10 min at 22°C in a volume of 700 μl. Extraction was performed after a second addition of fresh enzyme and an additional 10-min incubation period.

Crystallization

Stable-5-LOX S663D and Stable-5-LOX S663A crystals were grown by hanging-drop vapor diffusion at 295 K by mixing 1 μl protein (8 mg/ml) and 2 μl reservoir solution containing 8–10% Tacsimate, pH 6.0 (Hampton Research, Aliso Viejo, CA, USA). Crystals were also grown in an anaerobic chamber from Coy Laboratories (Grass Lake, MI, USA), and then soaked in 70% Tacsimate (pH 6.0) with 1 mg/ml AA for 3 h. Crystals were frozen in liquid nitrogen, if applicable inside an anaerobic chamber, for shipment and data collection.

Structure determination

Diffraction data were collected at 100 K at the NE-CAT beamline 24-ID-E at the Advanced Photon Source (Argonne, IL, USA). Data were processed with Xia2 (22). A monomer (unrestrained by noncrystallographic symmetry and stripped of water molecules) of the previously solved Stable-5-LOX structure (2.4 Å resolution), was used to position both chains in the asymmetric unit with Phaser (23). The molecular replacement solution was refined in Phenix to 2.1 Å (24). Clear density for the forked side chain of the S663D mutant (in the absence of substrate), as well as for the new position for D655, was evident in the F_o-F_c electron density map. In contrast, significant regions of the search model did not have main chain density in the $2F_o$-F_c electron density map calculated with data collected with AA-S663D crystals. These regions of the model were deleted, and the model was rebuilt over several cycles of manual rebuilding and refinement. Manual model building was performed with Coot (25). Further refinement in Phenix (24) was performed with individual atomic displacement factors (B factors) and automatic water picking. Illustrations were prepared with PyMOL (26). The PDB codes are 3V92, 3V98, 3V99 for the S663A, S663D, and S663D plus AA structures, respectively.

TABLE 1. *Kinetic parameters for Stable-5-LOX and its S663A and S663D mutants*

Enzyme	Substrate	K_m (μM)	k_{cat} (s^{-1})
Stable-5-LOX	AA	11 ± 0.02	0.30 ± 0.02
	DGLA	ND	ND
	NAGly	ND	ND
S663A-Stable-5-LOX	AA	42 ± 11	0.43 ± 0.06
	DGLA	ND	ND
	NAGly	ND	ND
S663D-Stable-5-LOX	AA	3.2 ± 0.3	0.85 ± 0.03
	DGLA	1.2 ± 0.2	0.42 ± 0.02
	NAGly	1.6 ± 0.6	0.51 ± 0.07

Values are presented as means ± SD. ND, not determined.

RESULTS

Catalytic activity of the Ser-663Asp mutant of human 5-LOX

S663D and S663A mutations in Stable-5-LOX were overexpressed in *E. coli* and purified as previously reported for Stable-5-LOX (19). Stable 5-LOX has been shown to a have K_m for substrate equivalent to the wild-type enzyme. When the production of HPETE by the S663D mutant was monitored by the absorbance at 238 nm, the rate of reaction was triple that of its parent enzyme, while the affinity for substrate (indicated by K_m) was enhanced (**Table 1**). HPLC analysis of the reaction products revealed that the S663D mutant produced 15-HPETE (**Fig. 1**), with 0 to at most 10% 5-HPETE in different incubations. Chiral HPLC analysis indicated that the product is exclusively the 15*S* enantiomer (data not shown). The S663D mutation in the context of the wild-type 5-LOX protein was also prepared and incubated with AA, and the products were analyzed by HPLC; the results of the analysis established that S663D-5-LOX also produces 15-HPETE. By contrast, the S663A mutant enzyme exhibits wild-type catalytic activity, forming 5-HPETE as the sole product; the maximal rate of reaction of the S663A mutant is similar to that of Stable-5-LOX, although the K_m for substrate is significantly higher (Table 1). It is difficult to make a direct comparison of the turnover numbers of the wild-type *vs.* Stable-5-LOX, as the latter enzyme has been engineered to have a longer half-life. Thus, as expected, the turnover rate for Stable-5-LOX is ≥10-fold improved over that for the fully activated wild-type enzyme (27).

Distinct differences exist in the fatty acid substrate specificities for 5-LOX and 15-LOX enzymes. While AA is the prototypic substrate for either isoform, 5-LOX is almost unreactive with linoleic acid, DGLA, or arachidonate derivatives bearing a bulky carboxyl ester or amide (28, 29), all of which are acceptable substrates for 15-LOX. Thus, it was of interest to examine the activity of the S663D mutant enzyme with these poor 5-LOX substrates. The results indicate that the S663D mutant efficiently oxygenated linoleic acid, DGLA, and NAGly at rates approximately equivalent to that for AA (Table 1). The products were identified after reduction of the hydroperoxides as 13*S*-hydroxylinoleate (only 1% 9-hydroxy), 15-hydroxy-DGLA, and the 15-hydroxy-*N*-Gly-20:4, respectively (data not shown). Thus, both of the eicosanoid substrates are accommodated in the active site so that C15, and not C5, is positioned to accept the peroxide group. S663D-Stable-5-LOX displays a robust catalytic activity with all of the typical 15-LOX substrates. Under the same conditions, Stable-5-LOX or its S663A mutant did not transform linoleic acid, DGLA, or NAGly at appreciable rates.

The potential for LX biosynthesis *via* modification at Ser-663

Biosynthesis of the anti-inflammatory LX mediators (*e.g.*, LXA, 5,6,15-trihydroxyeicosatetraenoic acid) is considered to involve the actions of multiple cell types and multiple LOX enzymes, hence the derivation of the name lipoxin from "lipoxygenase interaction" products. Our discovery of a means whereby a cellular 5-LOX might be transformed into a functional 15-LOX (potentially by phosphorylation at S663) opens the door to the production of LXs by 5-LOX and modified 5-LOX within a single cell. To mimic this possibility *in vitro*; *i.e.*, to see whether 5-LOX and its S663D mutant could synthesize LXs in the absence of a native 15-LOX, Stable-5-LOX and its S663D mutant were incubated together with AA. HPLC analysis of the products of the coincubation revealed a compound with elution time and UV spectra characteristic of a LXA_4 standard, formed together with other LX isomers (**Fig. 2**).

Crystallization of the stable-5-LOX mutant enzymes

To gain insights into the structural basis for the striking effects of the S663D mutation, the S663D and S663A proteins were crystallized in an anaerobic chamber under conditions described for Stable-5-LOX (19). The strict anaerobic conditions allowed exposure of the crystals to AA without inducing its transformation to product. In this way we could determine the crystal structures of the S663D mutant enzyme in the presence (2.25 Å) and absence (2.1 Å) of AA. In addition, the structure of the S663A protein was determined at 2.74

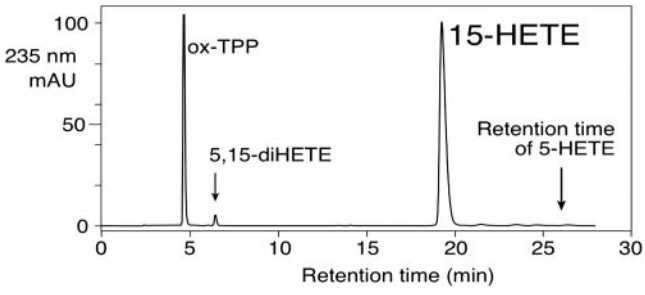

Figure 1. Product identification for S663D-Stable5-LOX. HPLC trace of the triphenylphosphine reduced product of AA oxidation by the S663D mutant of Stable-5-LOX.

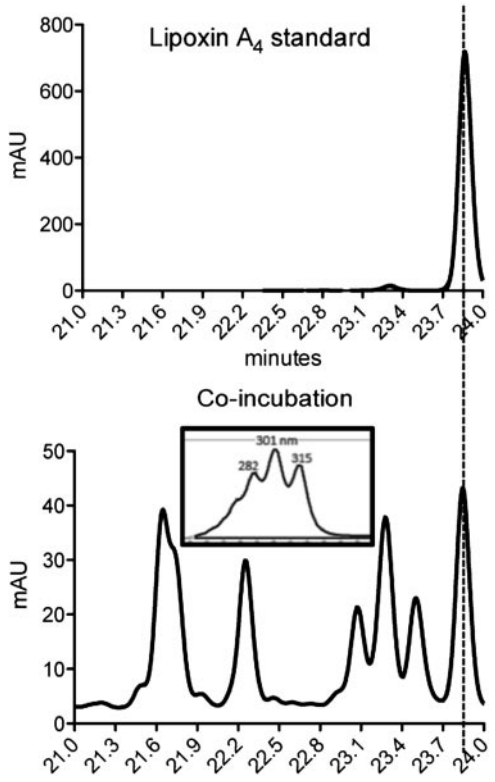

Figure 2. Coincubation of Stable-5-LOX and its S663D mutation with AA yields LXA_4. Top panel: elution profile for LXA_4 standard. Bottom panel: reversed-phase HPLC chromatogram of the analysis of the incubation mixture. LXA_4 is clearly distinguishable in the mixture of tri-HETE peaks observed by its retention time (23.85 min) and UV spectrum (inset); the nearby chromatographic peaks exhibit a similar UV chromophore and are LX stereoisomers.

Å resolution. The data and refinement statistics are given in **Table 2**.

Structures of the S663 mutant enzymes in the absence of AA

Significantly, in the absence of AA, the structures of both the S663D and S663A mutants are essentially unchanged from that of the parent enzyme Stable-5-LOX (rmsd 0.22 and 0.25 Å, respectively, **Fig. 3*A, B***). So, in the absence of substrate, the mutations have little effect on the overall structure. The structures display the general features typical of all LOXs, the N-terminal β-barrel domain, which in 5-LOX harbors the Ca^{2+} ions that promote membrane binding, and a larger α-helical domain where the catalytic iron resides (30–35). S663 is located 10 residues upstream of the C-terminal Ile that tucks into the catalytic domain helical bundle so that the free main-chain carboxyl can complete the iron coordination sphere characteristic of all LOXs. The elongated active site is sheltered by an arched helix and in Stable-5-LOX is "corked" at one end by the side chains of F177 and Y181. The opposite end is sealed by W147. Consequently, the active site cavity is not accessible to bulk solvent, and it is not obvious how substrate gains access to the catalytic machinery of 5-LOX.

Structure of the S663D mutant in the presence of AA

The structure obtained from crystals of S663D-Stable-5-LOX soaked in AA under anaerobic conditions revealed a difference in electron density attributable to AA in one of the monomers in the asymmetric unit (Fig. 3*C, D*) and dramatic AA-induced conformational changes in both monomers (**Fig. 4** and Supplemental Fig. S1). When the Stable-5-LOX structure is superimposed on that for the S663D mutant in the presence of AA, a total of 40 amino acids have no counterparts, and the RMSD for the remaining 630 is 0.46 Å (Fig. 4*A*). Four short polypeptide segments that are normally visible in the electron density map show no electron density in the AA-soaked crystal. These segments begin at amino acids 173, 189, 414, and 610 and include 4 amino acids that cover the active site (Fig. 4). The peptide that contains W605 and F610 (Fig. 4*B*) occupies a central position between the site of phosphorylation at 663 and the disordered peptides that define the active site in the apo structure. This region appears to be the communication hub that transduces a conformational change from S663 to the active site region.

The result of the remodeling in the AA-soaked crystal of S663D is a conspicuously accessible catalytic iron (Fig. 4*D*). The remodeling includes the reorientation of helical segments and disordering of extensive nonhelical and helical regions and results in an exposed active site, an open conformation. Two helices that normally help define the active sites of LOXs are helix-α2, which in 5-LOX is shorter and segmented relative to this element in other LOX structures, and an "arched" helix that contains a reverse turn insertion so that it curves away from the helical bundle to shelter an access channel to the catalytic iron (Fig. 4*A, D*). Both the segmented α2 and the arched helix undergo extensive remodeling in the presence of substrate. The loop (aa 171–176) that precedes the first segment of α2 is no longer visible in the electron density map, and the segment of helix itself is both shortened by three amino acids and slightly shifted. The next segment of α2 (aa 190–194) and the following 3-turn helix (aa 204–215) are fully displaced from their positions in the AA-free structure. Moreover, an extensive portion of the arched helix (from Leu-415 at the apex of the arch to its C terminus at 428) is not visible (Fig. 4*C*). The overall changes are summarized in Supplemental Fig S1.

Location of AA in the S663D crystal structure

As mentioned above, difference Fourier electron density (at 3 SD above the mean) attributable to a portion of AA is visible in one of the monomers of the asymmetric unit. (Both monomers display the conformational change described above.) A curved density, centered above the catalytic iron, that can encompass ~16 carbons of the substrate appears poised for attack (Fig. 3*C* and Supplemental Fig. S2). The partial density permits positioning of the substrate, but given that the AA is not restrained at either end by protein-substrate contacts (Fig. 3*D*), it is not possible to unambiguously determine its orientation in

TABLE 2. *Diffraction data and structure refinement*

Parameter	S663D mutant of Stable-5-LOX	S663D mutant of Stable5-LOX+ AA	S663A mutant of Stable-5-LOX
Data collection			
Space group	$P2_1$	$P2_1$	$P2_1$
Cell dimensions			
a, b, c (Å)	55.41, 202.50, 76.97	51.75, 200.84, 72.18	55.19, 202.38, 76.99
α,β,γ (deg)	90.00, 109.82, 90.00	90.00, 105.65, 90.00	90.00, 109.91, 90.00
Wavelength	0.97915	0.97915	0.979180
Resolution (Å)	49.38–2.07 (2.12–2.07)	35.57–2.25	49.35–2.74 (2.80–2.74)
$R_{p.i.m.}$	0.079 (0.345)	0.069 (0.350)	0.205 (0.370)
R_{merge}	0.114 (0.482)	0.077 (0.385)	0.267 (0.524)
$I/\sigma I$	6.0 (2.0)	9.8 (2.7)	5.9 (2.0)
Completeness (%)	99.8 (99.0)	94.3 (73.3)	98.9 (96.2)
Redundancy	3.6 (3.0)	2.9 (1.6)	3.3 (2.8)
Refinement			
Resolution (Å)	41.49–2.07 (2.12–2.07)	35.58–2.25 (2.31–2.25)	41.47–2.74 (2.80–2.74)
Reflections	91,112 (1983)	62,613 (2000)	41,033 (2061)
R_{work}/R_{free}	16.64/19.67 (22.66/25.63)	18.65/23.30 (23.49/31.75)	18.29/23.84 (29.23/34.44)
Atoms			
Protein	10,960	10,352	10,930
Water	956	392	161
Fe	2	2	2
B factors (Å^2)			
Protein	25.83	33.32	40.55
AA		74.37	32.97
Fe	11.90	17.61	
Water	29.62	36.83	27.14
Deviations (rms)			
Bond lengths (Å)	0.002	0.003	0.003
Bond angles (deg)	0.691	0.661	0.669
Ramachandran[a]			
Outliers (%)	0.0	0.1	0.0
Favored (%)	97.8	97.9	98.1

Values in parentheses are for the highest resolution shell; $R_{p.i.m.} = \Sigma_h [1/(n_h - 1)] \Sigma_l I_{hl} - I_h/\Sigma_{h\Sigma} \Sigma_l I_h$; $R_{merge} = \Sigma_h \Sigma_i |I_i - I_h|/\Sigma_h \Sigma_i I$; $R_{work} = \Sigma \|F_o| - |F_d\|/\Sigma |F_o|$, where F_o and F_c are the observed and calculated structure factor amplitudes, respectively. R_{free} was calculated using 3.2% of the total reflections. [a]Remaining residues lie in allowed regions.

the cavity. In Fig. 3*D* and Supplemental Fig. S2, the AA is positioned for attack at C13 to generate the 15*S*-HPETE, in agreement with the HPLC data.

DISCUSSION

S663 modification and LOX activity

Our results establish that the S663D mutation in human 5-LOX, with introduction of the Asp residue designed to mimic S663 phosphorylation (36, 37), results in a dramatic change in the specificity of oxygenation from purely 5*S* to almost purely 15*S*. It remains to be investigated how this relates to the actual phosphorylation of 5-LOX at S663, yet we can offer some arguments that support our interpretation that our results mimic a biologically relevant post-translational modification event. Paradoxically, a review of the literature on 5-LOX phosphorylation shows that generally it is inferred that 5-LOX phosphorylation at S663 is associated with enzyme activation; *i.e.*, the opposite of what our finding predicts. This inference is based on experiments in which the priming and subsequent stimulation of cells is associated with increased ERK1/2 activation, increased 5-LOX phosphorylation (that can be eliminated using the S663A enzyme, implying that it occurs at S663, and is blocked by ERK1/2 inhibitors), and, most strikingly, increased LT product formation. Although at first glance these observations support an activation role for phosphorylation at S663, some caveats are in order. Several parameters are altered when the cells are primed and stimulated. One is the phosphorylation, the extent of which is unknown, yet is quite likely to be low, perhaps only a few percent (38). Significant other factors are the increased supply of substrate (increased release of AA) and the enhanced 5-LOX translocation (16, 17, 39), both of which are optimized through cell priming and kinase activation, and both of which will increase product synthesis. Thus, while an associated 15-LOX activity has not been reported, these experiments were designed to measure the effect of 5-LOX phosphorylation on 5-LOX product formation in cells. They do not rule out the possibility of a subpopulation of 5-LOX that manifests a 15-LOX activity.

The crystal structures show that the S663D and S663A mutations have no effect on the overall protein fold, and the structures are almost indistinguishable from the parent Stable-5-LOX. Linoleic acid, DGLA,

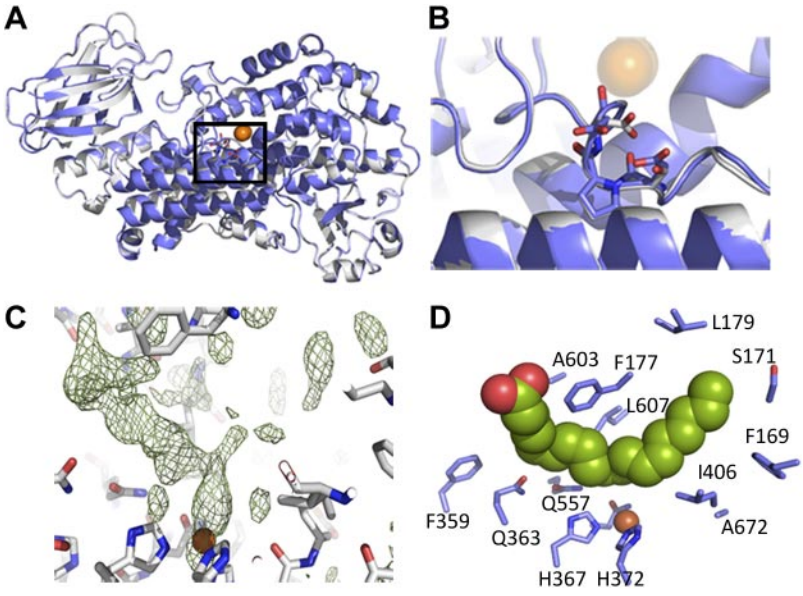

Figure 3. Comparison of the structures of Stable-5-LOX (gray) and the S663D mutant (blue). *A*) Cartoon rendering of the enzymes in the absence of substrate. Box indicates the region amplified in panel *B*. *B*) Detail at mutation: the negative charge of S663D results in a reorientation of D665. *C*) Difference density (at 3σ) apparent in the F_o-F_c map after molecular replacement and deletion of peptide regions where there is no electron density. Bulge emanating from the Fe is likely due to a water molecule positioned in the Fe coordination sphere for attack on the substrate. The long continuous density, with some broken pieces fthat complement it to reveal a U-shape, was interpreted as AA. *D*) AA as modeled in the refined structure. Amino acid side chains within 5 Å of the substrate are included.

and NAGly are poor substrates for 5-LOX but are readily oxygenated at the ω6 carbon (C15) by S663D-Stable-5-LOX. Linoleate and DGLA lack a pentadiene centered at C7 (which must align at the catalytic iron for attack for the production of 5-HPETE), and NAGly carries a bulky group at the carboxyl. None of these analogs are suitable 5-LOX substrates. The activity of the S663D mutant with these substrates, however, is consistent both with their identical structure to AA at the ω end of the carbon chain, as well as the predicted tail-first binding associated with 15-LOX activity (29). The implication of the tail-first binding is that the structural differences at the carboxyl end of the carbon chain have little effect on catalysis in the active site.

AA bound in the S663D enzyme

The structure determined with data obtained from crystals of the phosphorylation mimic S663D-Stable-5-LOX soaked in AA under anaerobic conditions re-

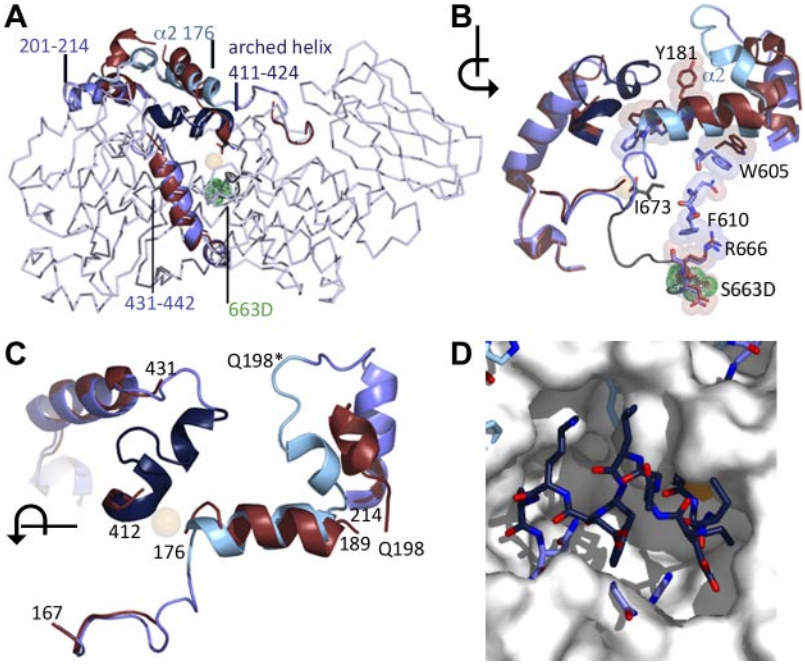

Figure 4. AA-induced remodeling (red) of the S663D phosphorylation mimic of Stable-5-LOX (blue; with the arched helix highlighted with dark blue coloring, and helix α2 in light blue). *A*) Stable-5-LOX Cα trace with cartoon rendering in the regions of remodeling. Shifts in helical placement as well as helix-to-disorder transitions are introduced across an extensive region of the protein. Arched helix is in dark blue; α2 (which is segmented) in light blue. Carboxyl group of the C terminus can be seen in the Fe (orange) coordination sphere. S663D is in green spheres, on the back side of the protein. *B*) Contact network of the S663D mutant of Stable-5-LOX (blue, sphere/stick rendering) that connects the site of phosphorylation (green) to the FY "cork" (Y181) that plugs the active site. View is from the back side of the protein as depicted in panel *A*. Arrow indicates the direction of rotation relative to *A*. Both F610 and W605 are positioned to play a role in transduction of the conformational changes. C-terminal Ile (I673; stick rendering) and the peptide backbone (gray cartoon) leading from S663 are in gray. Remodeled helical regions are depicted in cartoon rendering, colored as in panel *A*. Key remodeled residues are depicted in red sphere/stick rendering. In the presence of AA, Y181 can be seen popped open. *C*) Remodeled helices, rotated (arrow indicates direction of rotation relative to *B*) and viewed from above. Extent of AA-induced remodeling is significant in the area that defines the active site. Note the difference in position of Q198. Helical coloring as in panel *A*. *D*) Contours of the active site cavity are rendered as a white surface. Superimposed on the surface rendering is a stick rendering of the S663D mutant in the absence of AA. Note that the arched helix (dark blue), together with elements of α2 (light blue), covers this cavity and obstructs access.

vealed a dramatic substrate-induced conformational change. In this discussion, we refer to the "substrate-induced changes" in enzyme structure because AA is visible in one monomer of the asymmetric unit, yet both monomers exhibit structural alterations. The active site, which is completely inaccessible in the apo structures of Stable-5-LOX and its apo-S663A and S663D mutants, appears blown open; the highly conserved arched helix, present in all full-length LOX structures determined to date, is not visible in the electron density maps. The result is an unprotected catalytic site readily accessible to AA, and its analogs DGLA and NAGly.

Relation of structure to the altered catalysis

5-LOX produces 5*S*-HPETE, and the stereochemistry is consistent with the carboxyl end of the substrate lying at the end of the active site cavity closed by W147 (head-first rather than tail-first). The 15*S* product of the S663D is consistent with the inverse orientation, with the carboxylate at the FY cork end of the cavity (shown in Fig. 3*D* and Supplemental Fig. S2). Therefore, a simple reversal of substrate orientation in the cavity is all that is required to convert a 5-*S*-LOX to a 15-*S*-LOX; such an inversion is consistent with the product stereochemistry of S663D-Stable-5-LOX and LOX regiospecificity. Inversion of AA places C13 in the location of C7 to change the positional specificity of the enzyme and the stereochemistry of the product. The robust 15-LOX activity is supported by the improved kinetic parameters for the S663D mutant, and the distinctly open, and readily accessible, active site as a result of the substrate- induced conformational change described. Moreover, it is noteworthy that the highest turnover rates in the literature among LOXs are for the 15-LOX isoforms, as well as other LOXs predicted to bind substrate tail-first like 8R-LOX (40–42).

Detailed considerations of the structural changes

In the structure of Stable-5-LOX, S663 is at the amino terminus of a 3_{10} helix, and the side-chain -OH participates in an H-bond with the side chain of D665. With the addition of the negative charge at S663, D665 is nudged toward R666, which is in van der Waals contact with F610. In the presence of AA, the loop that contains F610 is not visible, and the helix that is just 2 residues upstream, the penultimate helix of the catalytic domain, is slightly shifted so that W605 bumps the first segment of the active-site-defining helix α2. As a consequence, the α2 segment is shifted relative to its position in the Stable-5-LOX (and the S663D- and S663A-mutant structures in the absence of AA). In addition, the arched helix is freed of the restraints that tether the C-terminal end by both repositioning of helices and order-to-disorder transitions in the vicinity. In effect, a network of H bonds and van der Waals contacts is disrupted by the presence of the negative charge, and this disruption impacts the locations of both α2 and the arched helix (Fig. 4*B–D*). Because it shelters the large catalytic site, the arched helix has limited contact within the catalytic domain; it is not adequately restrained to remain in position and enclose the active site.

The paucity of stabilizing contacts between the arched helix and the remainder of the catalytic domain was vividly illustrated by a structure of a truncated 12-LOX lacking the C2-domain (3D3L): neither α2 or the arched helix are positioned as they are in the full-length structures. The fragile nature of the intramolecular contacts between this active-site-defining helix results in a 5-LOX poised for a striking conformational change by the introduction of a negative charge distal to the active site. It appears that the introduction of a negative charge at position 663 allows substrate to trigger a large conformational change to expose an active site cavity and allow for its alternate positioning.

The potential for 5-LOX mediated LX biosynthesis and anti-inflammatory activity

We demonstrated here that LXA_4 is produced from coincubation of Stable-5-LOX and its S663D mutant. This result illustrates the possibility of the biosynthesis of LXs within a 5-LOX expressing cell in which native and modified enzyme might cooperate in the production of these trihydroxy anti-inflammatory mediators. Questions about the efficiency of such a system can be considered in comparison to the alternatives, including the current concept that cell-to-cell transfer of an intermediate is one of the pathways in the production of LXs. Notably, it was shown recently that depletion of eosinophils from mouse leukocytes, while abrogating 12/15-LOX activity, still allowed for significant production of both 15-HETE and LXA_4 (43). Our finding that Stable-5-LOX can be converted to a 15-LOX might explain this observation. FJ

This work was funded in part by grants from the American Heart Association (08553920E), the National Science Foundation (MCB 0818387), and the U.S. National Institutes of Health (NIH; HL 107887) to M.E.N. and from the NIH (GM-15431) to A.R.B. Preliminary work was performed at the Center for Advanced Microstructures and Devices (Baton Rouge), funded in part by the Louisiana Governors' Biotechnology Initiative. The work includes research conducted at the Advanced Photon Source on the Northeastern Collaborative Access Team beamlines, which are supported by grants from the National Center for Research Resources (5P41RR015301-10) and the National Institute of General Medical Sciences (8 P41 GM103403-10) from the NIH. Use of the Advanced Photon Source, an Office of Science User Facility operated for the U.S. Department of Energy (DOE) Office of Science by Argonne National Laboratory, was supported by the U.S. DOE under contract DE-AC02-06CH11357. Coordinates and structure factors have been deposited in the Protein Data Bank (3V92, S663A-Stable-5-LOX; 3V98, S663D-Stable-5-LOX; 3V99, S663D-Stable-5-LOX with AA).

REFERENCES

1. Evans, J. F., Ferguson, A. D., Mosley, R. T., and Hutchinson, J. H. (2008) What's all the FLAP about?: 5-lipoxygenase-activating protein inhibitors for inflammatory diseases. *Trends Pharmacol. Sci.* **29,** 72–78
2. Dixon, R. A., Diehl, R. E., Opas, E., Rands, E., Vickers, P. J., Evans, J. F., Gillard, J. W., and Miller, D. K. (1990) Requirement of a 5-lipoxygenase-activating protein for leukotriene synthesis. *Nature* **343,** 282–284
3. Radmark, O., and Samuelsson, B. (2009) 5-Lipoxygenase: mechanisms of regulation. *J. Lipid Res.* **50**(Suppl.), S40–S45
4. Shimizu, T., Radmark, O., and Samuelsson, B. (1984) Enzyme with dual lipoxygenase activities catalyzes leukotriene A4 synthesis from arachidonic acid. *Proc. Natl. Acad. Sci. U. S. A.* **81,** 689–693
5. Serhan, C. N., Hamberg, M., and Samuelsson, B. (1984) Lipoxins: novel series of biologically active compounds formed from arachidonic acid in human leukocytes. *Proc. Natl. Acad. Sci. U. S. A.* **81,** 5335–5339
6. Fiore, S., and Serhan, C. N. (1990) Formation of lipoxins and leukotrienes during receptor-mediated interactions of human platelets and recombinant human granulocyte/macrophage colony-stimulating factor-primed neutrophils. *J. Exp. Med.* **172,** 1451–1457
7. Edenius, C., Forsberg, I., Stenke, L., and Lindgren, J. A. (1991) Lipoxin formation in human platelets. *Adv. Prostaglandin Thromboxane Leukot. Res.* **21A,** 97–100
8. Ariel, A., Chiang, N., Arita, M., Petasis, N. A., and Serhan, C. N. (2003) Aspirin-triggered lipoxin A4 and B4 analogs block extracellular signal-regulated kinase-dependent TNF-alpha secretion from human T cells. *J. Immunol.* **170,** 6266–6272
9. Serhan, C. N., Chiang, N., and Van Dyke, T. E. (2008) Resolving inflammation: dual anti-inflammatory and pro-resolution lipid mediators. *Nat. Rev. Immunol.* **8,** 349–361
10. Folco, G., and Murphy, R. C. (2006) Eicosanoid transcellular biosynthesis: from cell-cell interactions to in vivo tissue responses. *Pharmacol. Rev.* **58,** 375–388
11. Werz, O., Klemm, J., Samuelsson, B., and Radmark, O. (2000) 5-lipoxygenase is phosphorylated by p38 kinase-dependent MAPKAP kinases. *Proc. Natl. Acad. Sci. U. S. A.* **97,** 5261–5266
12. Werz, O., Szellas, D., Steinhilber, D., and Radmark, O. (2002) Arachidonic acid promotes phosphorylation of 5-lipoxygenase at Ser-271 by MAPK-activated protein kinase 2 (MK2). *J. Biol. Chem.* **277,** 14793–14800
13. Werz, O., Burkert, E., Fischer, L., Szellas, D., Dishart, D., Samuelsson, B., Radmark, O., and Steinhilber, D. (2003) 5-Lipoxygenase activation by MAPKAPK-2 and ERKs. *Adv. Exp. Med. Biol.* **525,** 129–132
14. Luo, M., Jones, S. M., Flamand, N., Aronoff, D. M., Peters-Golden, M., and Brock, T. G. (2005) Phosphorylation by protein kinase a inhibits nuclear import of 5-lipoxygenase. *J. Biol. Chem.* **280,** 40609–40616
15. Flamand, N., Luo, M., Peters-Golden, M., and Brock, T. G. (2009) Phosphorylation of serine 271 on 5-lipoxygenase and its role in nuclear export. *J. Biol. Chem.* **284,** 306–313
16. Werz, O., Burkert, E., Fischer, L., Szellas, D., Dishart, D., Samuelsson, B., Radmark, O., and Steinhilber, D. (2002) Extracellular signal-regulated kinases phosphorylate 5-lipoxygenase and stimulate 5-lipoxygenase product formation in leukocytes. *FASEB J.* **16,** 1441–1443
17. Pergola, C., Dodt, G., Rossi, A., Neunhoeffer, E., Lawrenz, B., Northoff, H., Samuelsson, B., Radmark, O., Sautebin, L., and Werz, O. (2008) ERK-mediated regulation of leukotriene biosynthesis by androgens: a molecular basis for gender differences in inflammation and asthma. *Proc. Natl. Acad. Sci. U. S. A.* **105,** 19881–19886
18. Lee, Y. H., Olson, T. W., Ogata, C. M., Levitt, D. G., Banaszak, L. J., and Lange, A. J. (1997) Crystal structure of a trapped phosphoenzyme during a catalytic reaction. *Nat. Struct. Biol.* **4,** 615–618
19. Gilbert, N. C., Bartlett, S. G., Waight, M. T., Neau, D. B., Boeglin, W. E., Brash, A. R., and Newcomer, M. E. (2011) The structure of human 5-lipoxygenase. *Science* **331,** 217–219
20. Neau, D. B., Gilbert, N. C., Bartlett, S. G., Boeglin, W., Brash, A. R., and Newcomer, M. E. (2009) The 1.85 A structure of an 8R-lipoxygenase suggests a general model for lipoxygenase product specificity. *Biochemistry* **48,** 7906–7915
21. Studier, F. W. (2005) Protein production by auto-induction in high density shaking cultures. *Protein Expr. Purif.* **41,** 207–234
22. Winter, G. (2010) xia2: an expert system for macromolecular crystallography data reduction. *J. Appl. Crystallogr.* **43,** 186–190
23. McCoy, A. J., Grosse-Kunstleve, R. W., Adams, P. D., Winn, M. D., Storoni, L. C., and Read, R. J. (2007) Phaser crystallographic software. *J. Appl. Crystallogr.* **40,** 658–674
24. Zwart, P. H., Afonine, P. V., Grosse-Kunstleve, R. W., Hung, L. W., Ioerger, T. R., McCoy, A. J., McKee, E., Moriarty, N. W., Read, R. J., Sacchettini, J. C., Sauter, N. K., Storoni, L. C., Terwilliger, T. C., and Adams, P. D. (2008) Automated structure solution with the PHENIX suite. *Methods Mol. Biol.* **426,** 419–435
25. Emsley, P., and Cowtan, K. (2004) Coot: model-building tools for molecular graphics. *Acta Crystallogr. D Biol. Crystallogr.* **60,** 2126–2132
26. DeLano, W. L. (2002) The PyMOL Molecular Graphics System. http://www.pymol.org
27. Aharony, D., and Stein, R. L. (1986) Kinetic mechanism of guinea pig neutrophil 5-lipoxygenase. *J. Biol. Chem.* **261,** 11512–11519
28. Yamamoto, S. (1992) Mammalian lipoxygenases: molecular structures and functions. *Biochim. Biophys. Acta* **1128,** 117–131
29. Coffa, G., Schneider, C., and Brash, A. R. (2005) A comprehensive model of positional and stereo control in lipoxygenases. *Biochem. Biophys. Res. Commun.* **338,** 87–92
30. Boyington, J. C., Gaffney, B. J., and Amzel, L. M. (1993) The three-dimensional structure of an arachidonic acid 15-lipoxygenase. *Science* **260,** 1482–1486
31. Skrzypczak-Jankun, E., Amzel, L. M., Kroa, B. A., and Funk, M. O. (1997) Structure of soybean lipoxygenase L3 and a comparison with its L1 isoenzyme. *Proteins* **29,** 15–31
32. Gillmor, S. A., Villasenor, A., Fletterick, R., Sigal, E., and Browner, M. F. (1997) The structure of mammalian 15-lipoxygenase reveals similarity to the lipases and the determinants of substrate specificity [published erratum appears in *Nat. Struct. Biol.* **5,** 242]. *Nat. Struct. Biol.* **4,** 1003–1009
33. Choi, J., Chon, J. K., Kim, S., and Shin, W. (2008) Conformational flexibility in mammalian 15S-lipoxygenase: reinterpretation of the crystallographic data. *Proteins* **70,** 1023–1032
34. Oldham, M. L., Brash, A. R., and Newcomer, M. E. (2005) Insights from the X-ray crystal structure of coral 8R-lipoxygenase: calcium activation via A C2-like domain and a structural basis of product chirality. *J. Biol. Chem.* **280,** 39545–39552
35. Youn, B., Sellhorn, G. E., Mirchel, R. J., Gaffney, B. J., Grimes, H. D., and Kang, C. (2006) Crystal structures of vegetative soybean lipoxygenase VLX-B and VLX-D, and comparisons with seed isoforms LOX-1 and LOX-3. *Proteins* **65,** 1008–1020
36. Huang, W., and Erikson, R. L. (1994) Constitutive activation of Mek1 by mutation of serine phosphorylation sites. *Proc. Natl. Acad. Sci. U. S. A.* **91,** 8960–8963
37. Leger, J., Kempf, M., Lee, G., and Brandt, R. (1997) Conversion of serine to aspartate imitates phosphorylation-induced changes in the structure and function of microtubule-associated protein tau. *J. Biol. Chem.* **272,** 8441–8446
38. Radmark, O., and Samuelsson, B. (2010) Regulation of the activity of 5-lipoxygenase, a key enzyme in leukotriene biosynthesis. *Biochem. Biophys. Res. Commun.* **396,** 105–110
39. Flamand, N., Lefebvre, J., Surette, M. E., Picard, S., and Borgeat, P. (2006) Arachidonic acid regulates the translocation of 5-lipoxygenase to the nuclear membranes in human neutrophils. *J. Biol. Chem.* **281,** 129–136
40. Vliegenthart, J. F., and Veldink, G. A. (1982) Lipoxygenases. *Free Radic. Biol. Med.* **5,** 29–64
41. Borngraber, S., Grabenhorst, E., Anton, M., Conradt, H., and Kuhn, H. (1998) Intra- and extracellular expression of rabbit reticulocyte 15-lipoxygenase in the *Baculovirus*/insect cell system. *Protein Expr. Purif.* **14,** 237–246
42. Boutaud, O., and Brash, A. R. (1999) Purification and catalytic activities of the two domains of the allene oxide synthase-lipoxygenase fusion protein of the coral plexaura homomalla. *J. Biol. Chem.* **274,** 33764–33770
43. Yamada, T., Tani, Y., Nakanishi, H., Taguchi, R., Arita, M., and Arai, H. (2011) Eosinophils promote resolution of acute peritonitis by producing proresolving mediators in mice. *FASEB J.* **25,** 561–568

Received for publication January 27, 2012.
Accepted for publication April 10, 2012.